SUPPORTING INFORMATION

A production method under surveillance: Laboratory pilot-scale simulation of CH_4-CO_2 exchange in a natural gas hydrate reservoir

Katja Heeschen[1*]
Christian Deusner[2]
Erik Spangenberg[1]
Mike Priegnitz[1]
Elke Kossel[2]
Bettina Strauch[1]
Nikolaus Bigalke[2, 3]
Manja Luzi-Helbing[1]
Matthias Haeckel[2]
Judith M. Schicks[1]

Heeschen et al. (2021) Engery & Fuels; https://pubs.acs.org/doi/10.1021/acs.energyfuels.0c03353.

Number of pages: 7

Number of figures: 4

Number of tables: 0

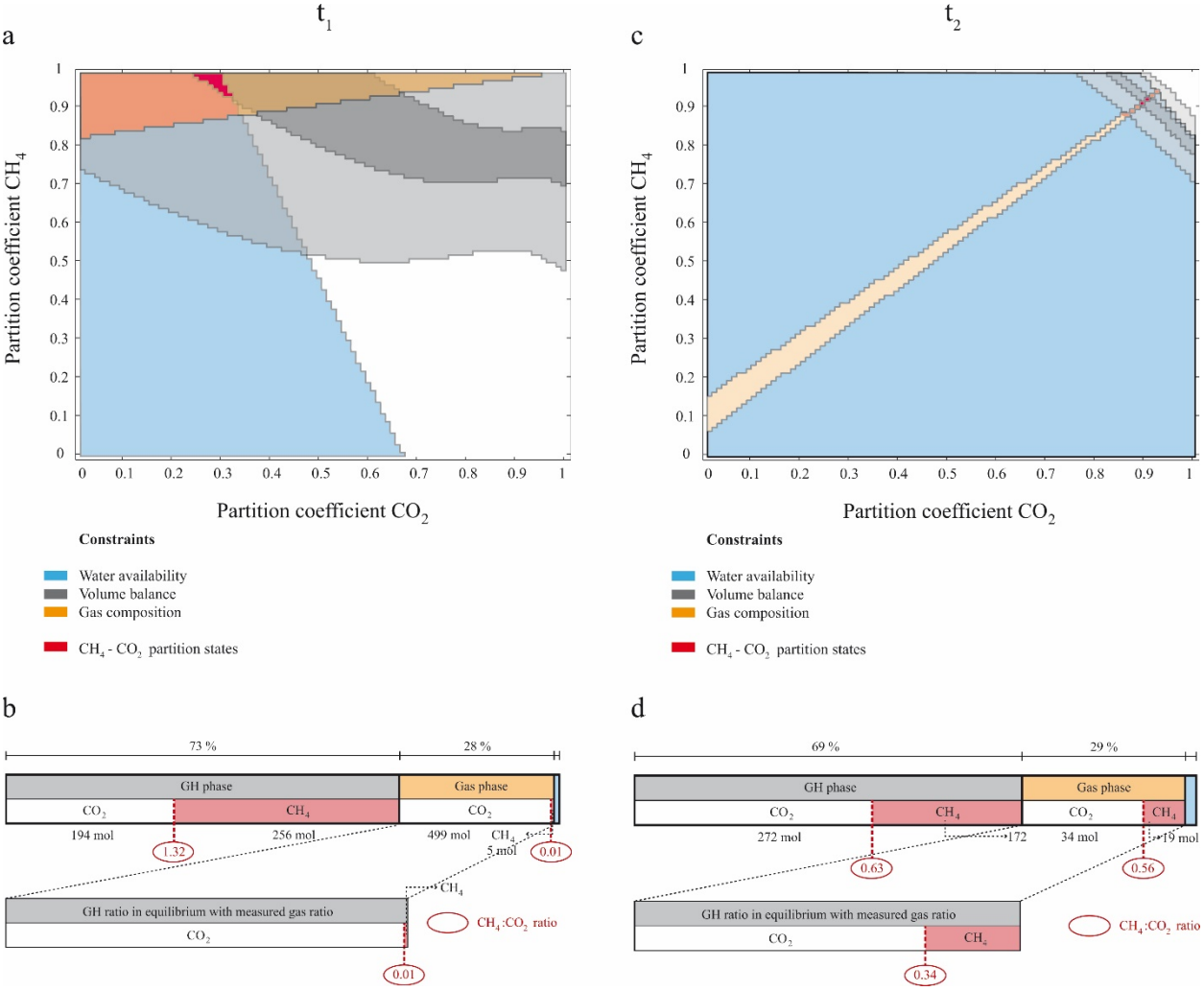

Fig. S1 Phase and component distributions during depressurization in E1; a) CH_4 and CO_2 distribution at t_1 (before depressurization) between a gas phase (partition coefficient = 0) and a gas hydrate phase (partition coefficient = 1); CH_4 and CO_2 distribution at given constraints (blue: water availability; grey: phase saturation; yellow: effluent gas composition); grey: possible CH_4:CO_2 partition states based on phase saturation constraints assuming an error of ± 2.5% ($S_w + S_g + S_{gh}$ = 0.975 to 1.025) (dark grey) or an error of ± 10% (light grey). The overlay of all given constraints results in overall possible CH_4 and CO_2 distributions as shown by red areas (Light red: Error ± 10%, bright red: Error ± 2.5%). b) Phase and component inventories based on possible partition states prior to depressurization at t_2 of experiment E1; Gas hydrate (GH) and gas phase CH_4:CO_2 ratios refer to the average of the bright red region for partitioning coefficients in the upper diagram

(upper bar chart); the lower bar chart shows the theoretical CH_4:CO_2 gas hydrate composition that would be in equilibrium with the detected gas phase; numbers in red show the CH_4:CO_2 molar ratios in the corresponding phase; c ,d) show the corresponding results at time t_2.

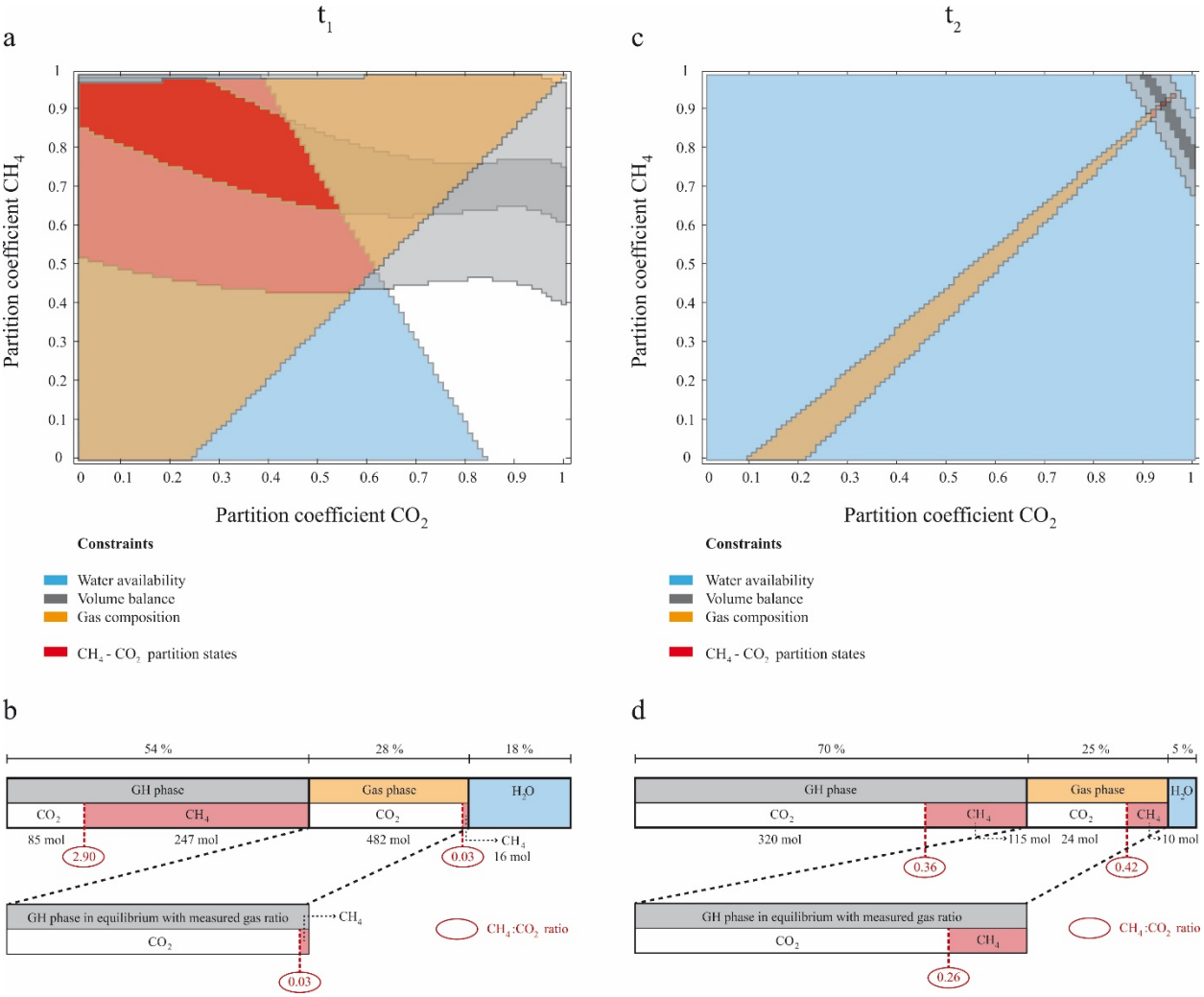

Fig. S2 Phase and component distributions during depressurization in E2; a) CH_4 and CO_2 distribution at t_1 (before degassing) between gas phase (partition coefficient = 0) and gas hydrate phase (partition coefficient = 1); b) Phase and component inventories based on overall possible partition states prior to depressurization at t_1 of experiment E2; For further details see Supplementary Fig. S1.

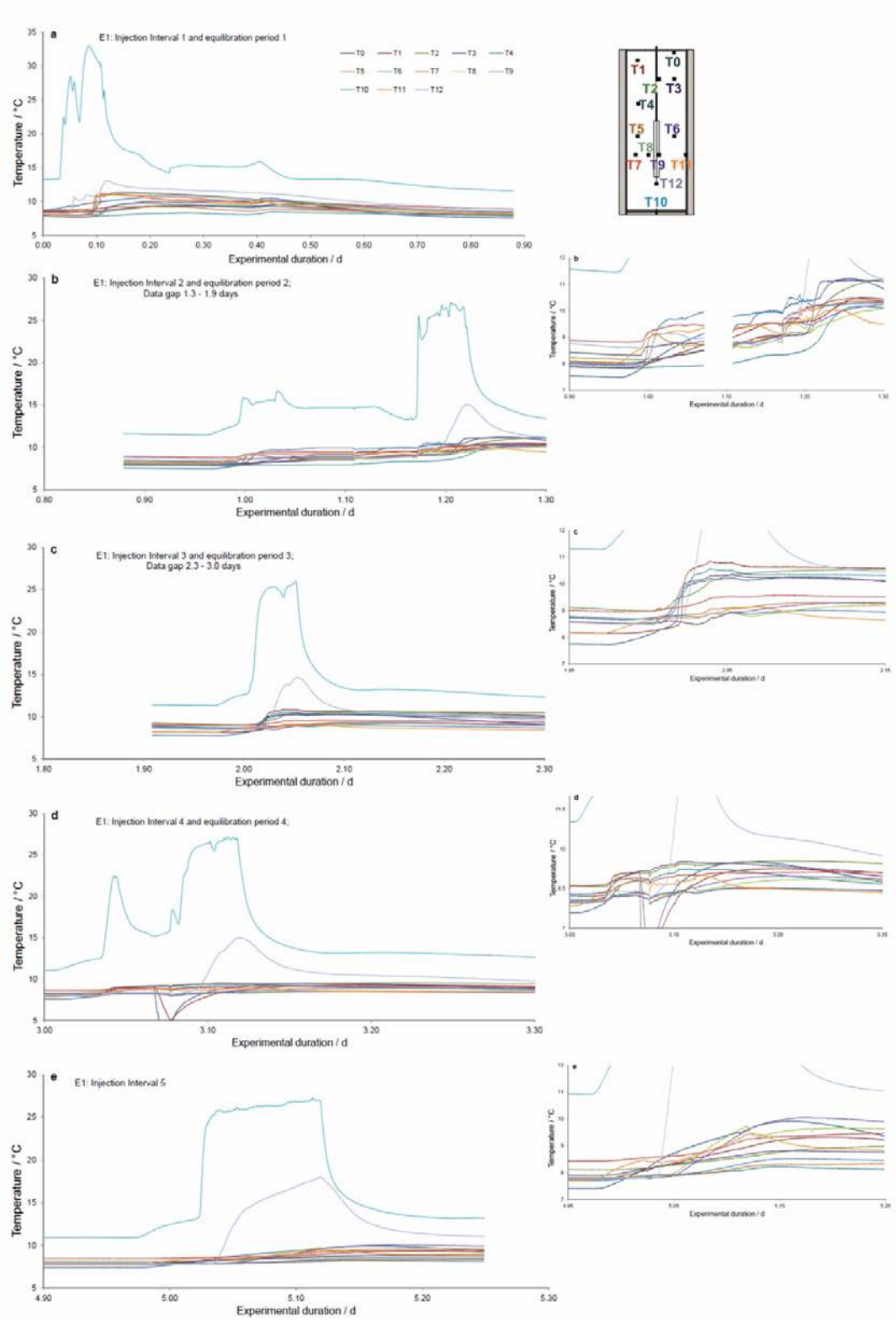
a
E1: Injection Interval 1 and equilibration period 1
T0 T1 T2 T3 T4
T5 T6 T7 T8 T9
T10 T11 T12
Temperature / °C
Experimental duration / d
T0
T1
T2
T3
T4
T5
T6
T8
T7
T9
T11
T12
T10
b
E1: Injection Interval 2 and equilibration period 2;
Data gap 1.3 - 1.9 days
Temperature / °C
Experimental duration / d
c
E1: Injection Interval 3 and equilibration period 3;
Data gap 2.3 - 3.0 days
Temperature / °C
Experimental duration / d
d
E1: Injection Interval 4 and equilibration period 4;
Temperature / °C
Experimental duration / d
e
E1: Injection Interval 5
Temperature / °C
Experimental duration / d

Fig. S 3 Temperature evolution during the five injection intervals and equilibration periods in experiment E1 (supplement to the top panel of Figure 5 in the main manuscript). While on the left the complete temperature ranges are plotted, the figures on the right show more detailed changes in the temperature range of 7 – 12 °C. In Fig. S3 d (injection interval 4) the negative excursion of temperatures in T0, T1 is due to a strong temporary pressure decrease (p= 3.5 MPa) at the outlet with subsequent degassing and gas hydrate decomposition.

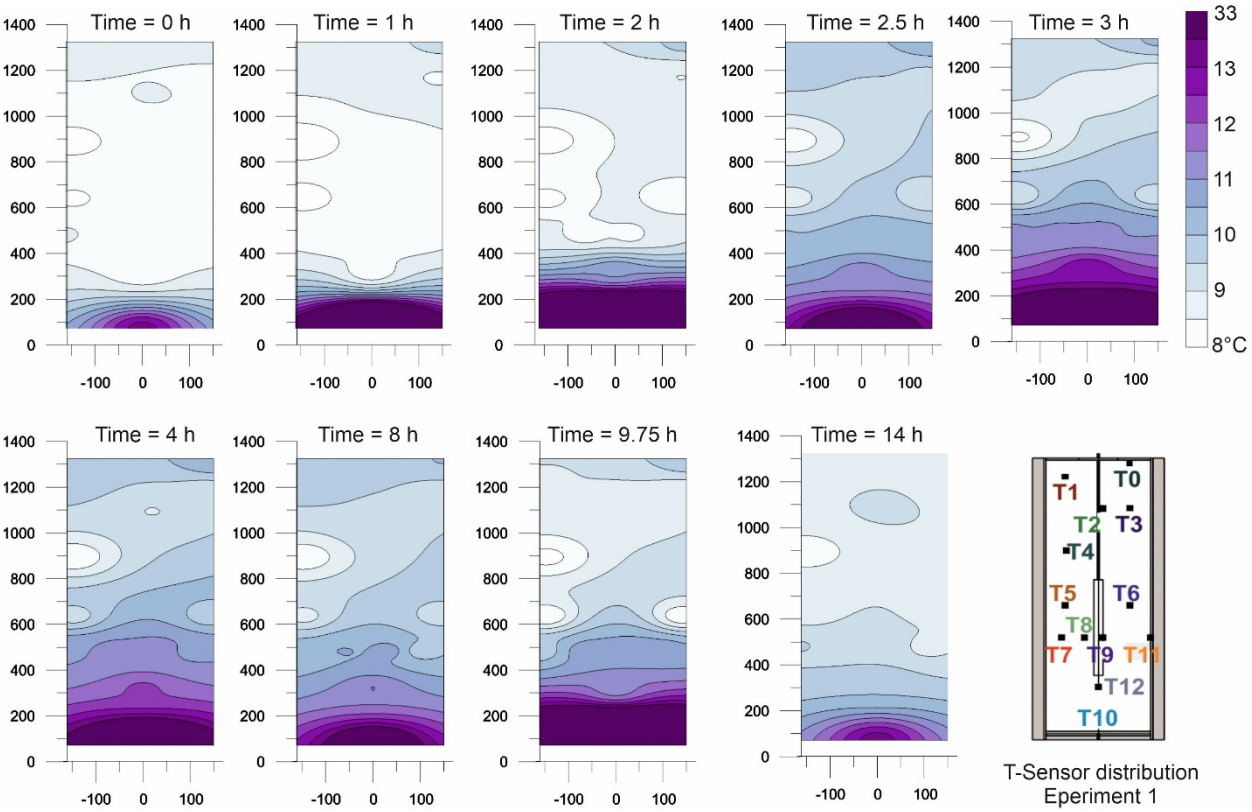

Fig. S 4 Temperature evolution during the first injection interval (0 – 4 h) and equilibration period (up to 14 h) of experiment E1 visualized as 2D - heat maps. Temperatures between 13.5 – 33° C are summarized in one color.